Nonlocal resistance and magnetoresistance in bulk metals

Mark Johnson* and R. H. Silsbee
Laboratory of Atomic and Solid State Physics, Cornell University, Clark Hall, Ithaca, New York 14853-2501
(Received 14 October 1988)

Sensitive voltage measurements are made on bulk metal wires with cross-sectional dimensions and probe separations L comparable to the electronic mean free path l. The voltage probes span a segment of the sample distinct from that carrying the current. For short l and $L \gg l$ the observed resistance and weakly parabolic magnetoresistance are consistent with a local conductivity analysis, $j=\sigma E$. However, when l is comparable to L, reproducible structure appears in the magnetoresistance. Neither the magnitude of the magnetic field characterizing the structure nor the decay length of the structure can be explained by the local-conductivity model. The results are inconsistent as well with the phenomenon of universal conductance fluctuations. Characteristics of this signal, their implications, and possible explanations are discussed.

I. INTRODUCTION

In the past few years, considerable interest has developed in the exploration of electronic transport in the regime in which electrode spacing L becomes comparable to important physical lengths in the system under study. These lengths include the elastic mean free path[1] $l=v_F\tau_{el}$, the inelastic diffusion length[2] $L_{in}=(D\tau_{in})^{1/2}$, the spin diffusion length[3] $L_s=(D\tau_s)^{1/2}$, and, in superconductors, the branch imbalance diffusion length[4] $L_{BI}=(D\tau_{BI})^{1/2}$. Here D is the electron diffusion constant and τ_{el}, τ_{in}, τ_s, and τ_{BI}, are respectively, the elastic, inelastic, spin lattice, and branch imbalance relaxation times. During the course of studies of the spin transport in aluminum,[3] in the regime $L \approx L_s$, magnetic-field-dependent signals were observed which were clearly demonstrated not to have their origin in spin coupling between injection and detection probes. A study was undertaken to define the physical origin of these signals and the results are presented herein.

The geometry of our experiment, a "standard four-probe measurement" with current provided through one pair of electrodes and voltage measured with a second pair, is *unconventional* (see Fig. 1). The voltage probes span a portion of the sample which, for our models of a material obeying a local conductivity law ($j=\sigma E$ with j a current density, $\sigma=1/\rho$ a local conductivity, and E the electric field), would contain no current; any measured voltage implies a violation of a local Ohm's law.

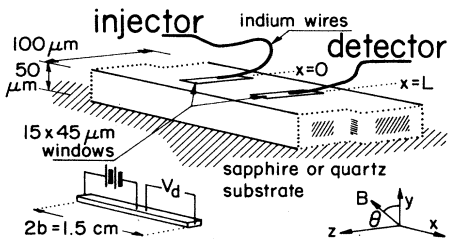

FIG. 1. The geometry of the experiment. The injector and detector are grounded at opposite ends of the wire, so that, classically, there should be no voltage drop across the detector. Some samples are oriented with the (100) crystal direction along $\hat{\mathbf{x}}$ and (010) along $\hat{\mathbf{y}}$. A magnetic field may be applied at angle θ in the y-z plane.

Two possible sources of nonlocality come to mind for the experiments described here. One is associated with the observation that $L \sim l$ implies a nonlocal response resulting from the ballistic nature of the transport; local response is expected only on length scales long compared with the elastic mean free path. A second is suggested by the fact that we also are in the regime with $L \sim L_{in}$, the regime of weak localization and of universal conductance fluctuations. In this regime, quantum interference may play an important role.

This paper summarizes the results of this investigation and discusses these results in the context of other magnetotransport work. Section II describes the experimental procedure and sample preparation, Sec. III presents results, and Sec. IV gives some analysis and discussion.

II. PROCEDURE AND SAMPLE PREPARATION

The sample geometry is depicted in Fig. 1, and described in detail elsewhere.[5] A small bar of bulk metal, about 50 μm by 100 μm by 1 cm, is fixed to a sapphire or quartz substrate and coated with an insulating film of polyimide. An array of windows, each 15 μm by 45 μm with spacing in multiples of 50 μm, is photolithographically defined and chemically etched through the imide, exposing the surface of the metal. The surface is cleaned with an argon-ion mill, and an array of gold films is evaporated such that each film overlaps a window. Indium wires leading to the injection and detection circuits are cold welded to these films. The detector used a sensitive SQUID (superconducting quantum interference device)[6] voltmeter to measure with picovolt sensitivity. The injected current is returned at one end of the bar, and the detector circuit is returned to the other end. Thus, in a one-dimensional model of the experiment, there is no net current upstream of the injector, and there should be no

voltage drop across the detector. It is possible, however, that injected electrons which propagate in the positive $\hat{\mathbf{x}}$ direction a distance of the order of the bulk mean free path could result in a nonzero voltage measured at the detector.

The metal primarily studied was aluminum. The bulk metal, originally 1 mm thick, had a residual resistivity ratio (RRR) at 4 K greater than 10 000. Using the constant[7] $\rho_b l_b = 9\times10^{-12}$ $\Omega\,\mathrm{cm}^2$ and a room-temperature resistivity $\rho_b = 2.7$ $\mu\Omega$ cm, the room-temperature bulk mean free path is found to be $l_b(295) = 330$ Å, and at 4 K, $l_b(4) > 330$ μm. Here $l_b = v_F(\tau_{\mathrm{imp}}^{-1} + \tau_{\mathrm{in}}^{-1})^{-1}$, where τ_{imp} and τ_{in} are the impurity and inelastic (phonon) relaxation times, respectively, refers to the mean free path associated with scattering in the interior of the sample. The bulk metal was cold rolled into progressively thinner sheets until 50-μm-thick foils were attained, and then annealed. Diffuse surface scattering causes a size effect in the resistivity of metal foils if the thickness of the foil is comparable to or smaller than the bulk electronic mean free path. Electron trajectories in the plane of the foil have the same mean free path as in a bulk sample, l_b, but those with velocity components transverse to the plane of the foil have mean free path limited by surface scattering. Analysis of $\rho(T)$ for our foils is consistent with other size-effect data[8] if the bulk mean free path is taken to be about 150 μm; we believe that the cold-rolling process induced some damage (perhaps in the form of impurities) in the aluminum, thereby diminishing l_b. Finally, thin wires were cut from the foils with a razor blade and were processed as described above. In a wire whose cross-sectional dimensions are comparable to, or smaller than, electronic mean free paths, electron trajectories along the axis of the wire have the same mean free path as in the bulk, l_b, but trajectories with velocity components transverse to the axis of the wire have mean free paths limited by surface scattering. The resistivity of our wires is analyzed by using the modified[9] Dingle formula, with the assumption of totally diffuse scattering of the electrons at the surface,

$$\frac{l_b}{l} = 1 + 0.23 l_b \frac{P}{A}\ , \tag{1}$$

where l is the observed (spatially averaged) mean free path in the wire, l_b is the deduced bulk value, and P and A are, respectively, the perimeter and area of the wire cross section. We find $l_b = 70$ μm; it is likely that cutting and processing the wires induced some additional damage to the aluminum and further diminished l_b.

The average dimension of a crystallite in the foil was 0.5 mm; for probe separations of 50–300 μm it is likely that most experiments were performed on single crystallites of unknown orientation. Some samples were cut from portions of the foil that had been etched with a mixture of phosphoric acid and aqua regia. Large crystallites were identified, their orientations were determined by the Laue method, wires were cut with the (100) axis of the crystallite approximately along the $\hat{\mathbf{x}}$ axis of the wire, and the probes were placed on the single, large crystallite.

In practice, the measurements are typically made at 4 Hz so that a lock-in can be used to reduce noise and drift. A bridge balances stray reactances in the detector circuit, and phase error in the bridge allows an uncertainty of a few tenths of a nΩ in the baseline of any curve. From day to day the baseline of a typical curve may vary by several tenths of a nΩ for unknown reasons.[10] However, the magnetic-field structure reproduces to an accuracy of 0.1 nΩ, regardless of differences in the baseline. Measurements have also been made at dc which reproduce the same structure and baseline as those taken ac. After many days and/or thermal cyclings, the detector circuit manifests a kind of switching noise at the 1–10-nΩ level and becomes unsuitable for further data collection.

III. RESULTS

The observed phenomenon is depicted in Fig. 2, which presents results from measurements on two, single-crystal wires. The series of plots from 2(a)–2(e) represents data for a single probe separation $L = 100$ μm and increasing electronic mean free path. This was achieved in the following way. One of the foils was etched, and then divided into two portions. Impurities were annealed into one of the portions in order to achieve an impurity limited, relatively short mean free path (deduced from the foil RRR of 600) of $l_b = 20$ μm. Wires were then cut and

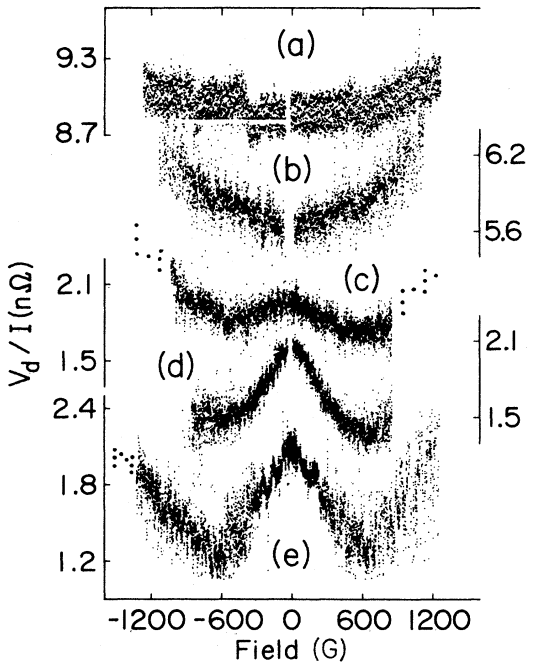

FIG. 2. The observed phenomenon, in oriented aluminum samples with $L = 100$ μm and a magnetic field applied along $\hat{\mathbf{y}}$. As the ballistic mean free path l_b approaches L, increasing from 20 μm in (a) to 70 μm in (e), reproducible structure emerges. Features of the structure vary with field and crystallographic orientation. The values l_b are determined from the temperature dependent resistivity of an identical wire and Eq. (1). (a) Sample Walr24 (impurities were added) at 4.3 K, $l_b = 20$ μm. Sample Walr40 at (b) 21 K, $l_b \approx 35$ μm; (c) 14.7 K, $l_b \approx 50$ μm; (d) 10 K, $l_b \approx 60$ μm; and (e) 4.3 K, $l_b \approx 70$ μm.

samples prepared, as described above, from both portions. In each experiment, a constant current I_{inj} is driven through the injector and the detector voltage V_d is digitized and recorded as the magnetic field is swept at a chosen angle θ (refer to Fig. 1). The resulting signals are linear with I_{inj} (for currents of 15–45 mA) and are presented as V_d/I_{inj}, in units of nΩ. The data presented in Fig. 2(a) are from the adulterated sample, which has the shortened mean free path. The zero field resistance is comparable to the prediction of a classical, local resistance model (presented below), and the weak, quadratic magnetoresistance of magnitude $\Delta R/R \approx 0.03$ is also consistent with the classical prediction for a sample with $(\omega_c \tau)^2 \approx 0.01$ where ω_c is the cyclotron frequency. These data are from a field sweep along the $\hat{y}$ axis, but are representative of field sweeps along any angle θ. The remainder of the curves in Fig. 2 are from the unadulterated sample. The field orientation is along the $\hat{y}$ axis for all curves. The temperature of the sample, for the data of Fig. 2(b), is 21 K; from the temperature dependence of an identical sample and from Eq. (1) the deduced bulk mean free path is $l_b \approx 35$ μm. Both the zero-field resistance is lower and the magnitude of the magnetoresistance is larger than for the sample of Fig. 2(a), as predicted by the classical model. The progression of curves presented in Figs. 2(b)–2(e) represents a monotonic decrease in temperature from 21 to 4 K, and a consequent monotonic increase in the deduced bulk mean free path from 35 to 70 μm. We observe the remarkable effect that as l_b increases further and approaches the probe separation L, structure emerges in the magnetoresistance, and the magnitude of the signal increases, rather than continuing to decrease. This structure reproduces from day to day and run to run (i.e., after warming). It has been observed in seven probe pairs on five different wires, for all orientations θ of field.

Figure 3 is another presentation of the phenomenon, in a manner that demonstrates some important characteristics. Here the approach to the limit $l_b \sim L$ is performed by decreasing the interprobe spacing L. These measurements were performed on unoriented crystallites of polycrystalline wires at four different probe spacings. In this series the temperature is approximately constant (about 4 K), and the progression [3(a)–3(d)] represents probe separations decreasing from 300 to 50 μm. Two important characteristics of the signal are apparent from this sequence: Both the width and the amplitude of the feature decrease with increasing probe separation. The following observations are also noteworthy. In Fig. 3(d), the resistance becomes negative for fields larger than a few hundred Gauss. The uncertainty in the baseline for this particular curve was 0.5 nΩ; thus the negative "resistance" is a real effect. In Fig. 3(c) the magnetoresistance shows two maxima (a third maximum in positive fields has been omitted from the plot). Two of the six probe pairs on aluminum wires (at $L = 100$ and 200 μm) showed more than one maximum. Of the remaining four pairs, it is likely that two show only a single maximum [those represented in Figs. 3(a) and 3(b)], while the other two [those represented in Figs. 2 and 3(d)] were not studied with sufficient field ranges to determine whether more than a single maximum exists. Finally, we note that a maximum need not be centered exactly at $B = 0$.

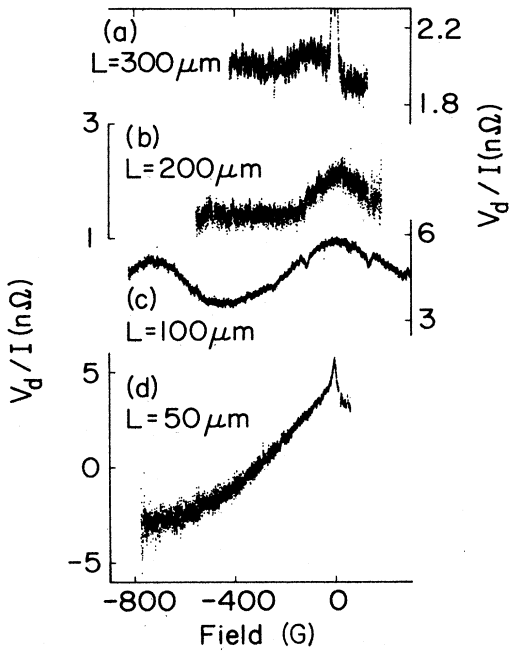

FIG. 3. Approaching the regime $l_b \sim L$ by successively decreasing L. These examples of the phenomenon are from unoriented crystallites of polycrystalline wires. (a) $L = 300$ μm, 4.3 K; (b) $L = 200$ μm, 4.3 K; (c) $L = 100$ μm, 6.9 K; and (d) $L = 50$ μm, 13 K. The uncertainty in the zero-field value (equivalently the baseline) is less than 0.5 nΩ for (d), where negative "mutual" resistance is observed. The narrow feature at zero field in (a) and (d) is from spin-polarized electrons, and is reported elsewhere (Ref. 3). The "glitches" in (c), as well as in Fig. 2(a), are spurious effects of cerralow solder connections undergoing a superconducting transition. In (c) and (d) the amplitude is essentially the same at lower temperatures; these curves were chosen because of lower noise and larger field range.

The observation of decreasing feature amplitude with increasing probe separation L is treated in Fig. 4(a), which is a semilog plot of the amplitude, at constant temperature, as a function of L for the unoriented crystallites of Fig. 3. The amplitude is taken to be the difference, for a given magnetoresistance curve, between signal maximum and minimum. There are variations of amplitude for different orientations θ. The plot includes data for several different orientations[11] near perpendicular field, and for two probe pairs at $L = 200$ μm. The straight line represents the fit

$$R = (14\ \text{n}\Omega) e^{-L/\Lambda} ,$$

where the decay length is $\Lambda = 70$ μm.

As noted above, it can be seen in Fig. 3 that the feature width in magnetic field scales approximately as $1/L$. As a function of orientation angle θ, the width for constant L can vary by 50%, which makes generalizations tenuous at best. However, for the sake of analysis, the "period" B_λ is defined to be the difference in field between signal

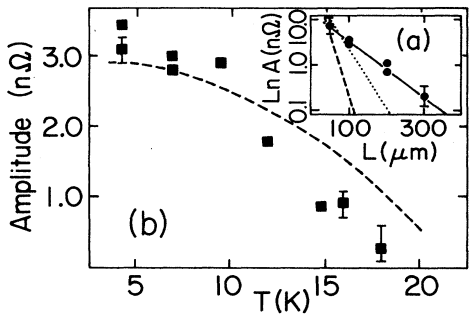

FIG. 4. (a) Semilogarithmic plot of the average amplitude as a function of probe spacing L, at 4.3 K, for unoriented crystallite on polycrystal wires. The nonlinear least-squares fit was (14 $n\Omega$)$e^{-L/\Lambda}$, where $\Lambda=70$ μm. The dashed and dotted lines are predictions of local resistivity models. (b) The temperature dependence of the amplitude for fixed L (100 μm). The dashed line is the function (14 $n\Omega$)$e^{-(100\ \mu m)/l_b(T)}$.

maxima in Fig. 3(c), and twice the approximate difference in field from signal minimum to maximum for the other curves. We observe the approximate scaling

$$B_\lambda L=\text{const}=\Phi_0/\alpha\ , \tag{2}$$

where $\Phi_0=hc/e=4.2\times10^{-7}$ G cm^2, and α is about 6 Å for the data set of Fig. 3. The structure width, for given L and θ, does not change with temperature, at least up to those temperatures for which there is adequate signal to noise to distinguish the feature.

For constant L and θ, the signal amplitude as a function of temperature is presented in Fig. 4(b). Here $L=100$ μm, and the measurements were on an unoriented crystallite [i.e., from the same data set as Fig. 3(c)]. Other data sets show similar behavior. The dashed line is the function (14 $n\Omega$)$e^{-(100\ \mu m)/l_b(T)}$, where $l_b(T)$ was measured[12] in aluminum of comparable purity. It should be noted that the phase length, $L_\phi=(D\tau_{in})^{1/2}$, in our samples is about 200 μm at 4 K. Here we have used a value of the diffusion constant $D(T)$ measured on an identical sample, and the value $\tau_{in}(4\ K)=3\times10^{-9}$ sec is estimated from the work of other authors.[13] In a standard model,[13] τ_{in} varies as T^{-3}, so that L_{in} has diminished to $L_\phi=55$ μm at $T=9.5$ K. Thus, for the data in Fig. 4(b) we see that the ratio of probe separation to phase length L/L_ϕ goes from ~0.5 to ~2 in the temperature range of 4–9.5 K, yet the amplitude of the effect is essentially unchanged over this same temperature range.

IV. ANALYSIS AND DISCUSSION

The observation of a signal in a portion of the sample far upstream from the segment of the wire that carries the current is not consistent with a classical, local resistance. In a one-dimensional model, the detector circuit should detect zero resistance. For a real three-dimensional sample there can be signals detected upstream of the injecting probe even in the local conductivity limit. Near a point injecting probe, the current is isotropic over a hemisphere, equal amounts starting upstream and downstream; fields $E=\rho j$ will therefore exist upstream. These fields fall off exponentially, however, with a characteristic length of the order of the sample cross-sectional dimensions, and may be easily modeled. It is proposed that these fields indeed give rise to the signal [see Fig. 1(a)] in the high-resistivity sample. To estimate the magnitudes of these signals, three idealized geometries are discussed. In model I it is assumed that all the current I_{inj} enters the bar of width a at the center of the injection window, $z=0$. An equivalent problem, with Fourier expansion solution, is a two-dimensional array of δ-function injectors on a semi-infinite foil, of length $2b$, in the x-z plane:

$$\nabla\cdot\mathbf{j}(x,z)=[-1/\rho_s(T)]\nabla^2V(x,z)$$
$$=I_{inj}\delta(z-ma)\delta(x)\ ,$$

where $m=0,\pm1,\pm2,\ldots$. Here the injectors are in the middle of the foil, $x=0$, a ground plane is at $x=-b$, $\rho_s(T)$ is the resistance per square of the foil, and the detector voltage is $V_d=V(L,z)-V(b,z)$. The maximum value of V_d is at $z=0$

$$r_m(L)=\frac{V_d}{I_{inj}}=\sum_{n=1}\frac{\rho_s(T)}{2\pi n}e^{-2\pi nL/a}\ . \tag{3}$$

This "mutual" resistance is a measure of the penetration, in the bar, of the electric field due to the injector. It is sketched in Fig. 4(a) as a dashed line, and has a limiting decay length of $a/2\pi=16$ μm. In model II it is assumed that the current injection and signal detection occur uniformly along lines that span the width of the bar at $x=0$ and $x=L$, and the electric field penetrates up the bar because of its finite thickness. We consider a cross section in the x-y plane of the bar of thickness t, and solve the equivalent problem of an array of δ-function injectors $2I_{inj}\delta(y-2mt)\delta(x)$, where $y=0$ is at the top of the bar and m is as before. Noting that $a=2t$ for our samples, the solution happens to be numerically the same as model I. In model III, all current is assumed to be injected at a corner of the injection window, at $x=0$, $z=25$ μm (the 45-μm-long windows are placed with 5 μm accuracy). The maximum mutual resistance in this worst-case model (for a detector at $x=L$) is at $z=25$ μm and is sketched in Fig. 4(a) as a dotted line. The approximate decay length is $a/\pi=32$ μm. Recall that the decay length of the observed signal is about 4.5 times longer than that of model I, Eq. (3), and more than twice as long as the worst case model. Thus, the observed signal amplitudes are 10–1000 times larger than classical predictions at $L=200$ μm, and 10^2–10^5 times too large at $L=300$ μm. Further evidence against a local model as the source of the low-temperature signals are the observations that the theoretical decay lengths are defined by the geometry, not by the sample resistivity, and hence should be temperature independent; and that the signal is predicted to be proportional to the sample resistivity, and hence should decrease with decreasing temperature. The observations, however, clearly show an increasing signal amplitude and

increasing decay length with decreasing temperature, in contradiction with the predictions of the local theory.

Since the probe separation L is comparable with the inelastic length $L_{\rm in}$, it is natural to ask whether the signals are related to the universal conductance fluctuations which have received so much recent attention.[2] It is important to recognize a key experimental difference between our system and work on universal conductance fluctuations, which is typically performed on quasi-one-dimensional systems. Linewidths of typical GaAs/AlGaAs "wires" are of order 1000 Å. Because the Fermi wavelength is of order a few hundred Å, this width contains only a few "conductance channels."[14] Even metal lines that are of order 1000-Å wide and 100-Å thick contain only the order of 1000 "channels." We also note that, at low temperatures, the phase length of these systems can be of order 1 μm, so that the transverse dimensions are much smaller than a phase length. By contrast, our samples are typically 50×100 μm in cross section. With a Fermi wavelength of a few Å, our samples contain on the order of 10^{10} channels. Furthermore, at 4 K the cross-sectional dimensions of our samples are comparable to, but not smaller than, the phase length and ballistic length. At higher temperatures the dimensions are larger than $L_{\rm in}$ and l_b.

We believe our signals are not related to universal conductance fluctuations. (1) Noting that the probe spacing L and the sample cross-sectional dimensions are both comparable with the inelastic length $L_{\rm in}$ suggests[15] an expected conductance fluctuation signal of the order of

$$\Delta R=\frac{\Delta V}{I}=\frac{e^2}{h}\frac{L_{\rm in}^2}{w^2}R^2\sim10^{-18}\ \Omega\ ,$$

where w is the sample width and R the resistance per square of the sample, to be compared with the experimentally observed values of order 10^{-9} Ω. These samples have such a high conductance that one could hardly be expected to be able to observe the quantum conductance fluctuations. (2) One would expect the quantum interference to be altered by an applied magnetic field of the order of the coherence field defined by

$$B_c\approx\Phi_0/wL_{\rm in}\sim10^{-3}\ \text{G}\ .$$

In contrast, the magnetic fields required to give changes in the experimental nonlocal voltages are of the order of hundreds of G. (3) Figure 4(b) gives the temperature dependence of the signal amplitude for a probe separation $L=100$ μm. Using a T^{-3} dependence of $\tau_{\rm in}$ with $\tau(4\ \text{K})=3\times10^{-9}$ sec and a diffusion constant deduced from the conductance measured on an identical sample allows estimates of the diffusion length $L_{\rm in}$ at temperatures of 4 and 9.5 K. The calculated $L_{\rm in}$ changes from 200 to 55 μm (the ratio $L/L_{\rm in}$ changes from 0.5 to 2), yet the amplitude of the effect is essentially unchanged.

There appears no basis for associating the nonlocal signals with present pictures of "universal conductance fluctuations." Similar arguments dismiss weak localization as a plausible starting point to try to explain the observations.

In analyzing the characteristics of the effect, the observation that the decay length of the amplitude at 4 K [Fig. 4(a)] is essentially the same as the bulk mean free path deduced from Eq. (1), $\Lambda(4\ \text{K})=70\ \mu\text{m}\approx l_b(4\ \text{K})$, and the similarity between the plots in Fig. 4(b) suggest that the signal may be a ballistic electron effect. We have been unable, however, to construct a satisfactory model in terms of which to explain the results. Rough arguments may be given for the magnitude of the expected signal, which are in accord with the experiment; but a serious difficulty is in understanding the initially attractive correspondence evident in Fig. 4(a). With the assumption of diffuse reflection at the surfaces, as suggested by the sample dependence of the residual resistivity, one expects an amplitude dependence of the form $(1/L^2)e^{-L/\Lambda}$, where the prefactor $(1/L^2)$ is a consequence of the solid angle presented by the cross sectional area at the detector as seen from the vicinity of the source. Fits of the data to such a prediction are much worse than those of Fig. 4(a). The simple exponential dependence implied by the fit would suggest that the electrons propagate up the wire as a quasi-one-dimensional wave: $\Psi\sim e^{ikx}e^{-x/2l_b}$. A model which assumes specular rather than diffuse boundary scattering avoids the $1/L^2$ problem, but then the mean free path deduced from the decay length of the ballistic signal should correspond to the resistivity mean free path; since these lengths differ at 4 K by a factor of 4, the difficulty is not satisfactorily resolved.

Further difficulties arise as we speculate about possible mechanisms for the magnetic-field structure. The characteristic width of the feature is too small to be associated with free-electron cyclotron orbits. The cyclotron radius of an electron is $r_c=v_F/\omega_c$ where v_F is the Fermi velocity. In aluminum[16] $\omega_c=(2\pi/1.6)2.8$ MHz/G, so that for fields B in gauss the radius is $r_c=(18/B)$ cm. Thus, there is insufficient curvature from the Lorentz force in the small fields used to form a satisfactory model of a Shubnikov–de Haas effect, or of magnetic focusing.[17] Furthermore, the observation of the structure for all orientations θ suggests that the Lorentz force alone cannot be responsible for its existence. There is marked asymmetry in the structure, about $B=0$, for fields applied along $\hat{\mathbf{z}}$, as is expected for the symmetry of the sample defined by having both injector and detector on the same side of the wire.

Aluminum is trivalent, the Fermi surface is complicated,[18] and unusual effects could arise from cyclotron orbits of higher zone electrons. To learn whether the effect is peculiar to aluminum, a gold sample of comparable dimensions (25 μm by 90 μm by 1 cm), purity, and bulk mean free path was prepared. The probes were placed on a single, unoriented crystallite. Magnetoresistance structure qualitatively similar to that in the aluminum was observed, of appropriate magnitude ($\sim$ 7 nΩ at $L=50$ μm) and field width. Because gold is a nearly-free electron metal, it's not likely that the existence of the structure is due to obscure features of a Fermi surface. However, comparison of data for a (100) crystallite [Fig. 2(e)] and for an unoriented crystallite [Fig. 3(c)] suggests that the Fermi surface and band structure may determine specific characteristics of the feature.

The observation that the signal is sometimes periodic and the result from Eq. (2) that $B_\lambda L = \Phi_0/\alpha$ are suggestive of a possible quantum-mechanical interpretation[19] in which interference somehow occurs between trajectories separated by distance α. A Fermi wavelength or a lattice constant are both of the same order as the observed value of α. Limited results for field sweeps along the $\hat{\mathbf{x}}$ axis show no magnetoresistance structure, which is consistent with an interference model. However, no satisfactory theory yet exists.

We have reported the observation of a new magnetoresistance signal in bulk, high-purity metals in the regime with probe spacing comparable with the conductance mean free path and with the inelastic diffusion length. The data are grossly inconsistent with both a classical local conductance model and with simple ideas of universal conductance fluctuations. Some features of the results are suggestive that there are ballistic effects, i.e., deviations from a local Ohm's law consequent on the comparable magnitude of the probe separation and the conductance (elastic) mean free path, but no fully satisfactory explanation is developed.

ACKNOWLEDGMENTS

The authors are grateful to S. Hershfield for useful conversations and comments, and to H. Hurdequint for providing the gold foil. This work has been supported by the Cornell University Materials Sciences Center, through National Science Foundation Grant No. DMR-85-16616. We also acknowledge partial support by the Program on Submicron Structures and the National Resource and Research Facility for Submicron Structures (now, the National Nanofabrication Facility), Ithaca, NY.

---

*Present address: Department of Physics, University of California, Berkeley, CA 94720

[1]For example, a study of microbridges of single-crystal metals is given by E. E. Vdovin *et al.*, Zh. Eksp. Teor. Fiz. **92**, 1026 (1987) [Sov. Phys.—JETP **65**, 582 (1987)]; and studies of "wires" fabricated on $GaAs/Al_xGa_{1-x}As$ heterostructures are found in G. Timp, A. M. Chang, P. Mankiewich, R. Behringer, J. E. Cunningham, T. Y. Chang, and R. E. Howard, Phys. Rev. Lett. **59**, 732 (1987); G. Timp *et al.*, *ibid.* **60**, 2081 (1988); D. A. Wharam *et al.*, J. Phys. C **21**, L209 (1988).

[2]Examples of weak localization and Aharanov Bohm oscillations in metallic cylinders are found in D. Yu Sharvin and Yu V. Sharvin, Pis'ma Zh. Eksp. Teor. Fiz. **34**, 285 (1981) [JETP Lett. **34**, 272 (1981)] and N. B. Brandt *et al.*, Fiz. Nizk. Temp. **8**, 718 (1982) [Sov. J. Low Temp. Phys. **8**, 358 (1982)]; examples of Aharanov-Bohm oscillations in metal rings are found in R. A. Webb *et al.*, Phys. Rev. Lett. **54**, 2696 (1985); V. Chandrasekhar *et al.*, *ibid.* **55**, 1610 (1985); C. P. Umbach *et al.*, *ibid.* **56**, 386 (1986); C. P. Umbach, *et al.*, Appl. Phys. Lett. **50**, 1289 (1987); and examples of "universal conductance fluctuations" are found in C. P. Umbach *et al.*, Phys. Rev. Lett. **53**, 4048 (1984); D. Stone, *ibid.* **54**, 2692 (1985); W. J. Skoçpol *et al.*, *ibid.* **58**, 2347 (1987); and W. J. Skoçpol *et al.*, *ibid.* **56**, 2865 (1986). Finally, see also the excellent review by R. A. Webb *et al.*, Jpn. J Appl. Phys. **26**, 1926 (1987).

[3]Mark Johnson and R. H. Silsbee, Phys. Rev. Lett. **55**, 1790 (1985).

[4]Mark Johnson and R. H. Silsbee, Phys. Rev. Lett. **58**, 2806 (1987).

[5]Mark Johnson and R. H. Silsbee, Phys. Rev. B **37**, 5326 (1988).

[6]Commercial SQUID from B.T.I.

[7]Empirical values of $\rho_b l_b$ for aluminum, taken from size effect experiments, vary from 5×10^{-12} to 14×10^{-12} $\Omega\,\mathrm{cm}^2$. We have chosen a typical value, in the middle of the range. See Jack Bass, *Landolt-Börnstein, Numerical Data and Functional Relationships in Science and Technology, Group III* (Springer-Verlag, Berlin, 1982), Vol. 15a; J. R. Sambles and K. C. Elsom, J. Phys. F **10**, 1487 (1980).

[8]J. R. Sambles, K. C. Elsom, and G. Sharp-Dent, J. Phys. F **11**, 1075 (1981).

[9]L. R. Kirkland and R. L. Chaplin, J. Appl. Phys. **42**, 3054 (1971).

[10]Data represented in Figs. 2(a) and 3(c) had larger baseline deviations, on a day-to-day basis, of a few $n\Omega$.

[11]The amplitude can vary by a factor of 3 over the full angular range of 180°. The amplitudes presented in Fig. 4(a) are from orientations within 20° of perpendicular field.

[12]We have used $\rho_b l_b = 9\times10^{-12}$ $\Omega\,\mathrm{cm}^2$, and Fickett's measured values of $\rho_b(T)$ for bulk aluminum with an RRR of 2000, which is essentially the same as the deduced value of RRR (1900) for our aluminum (after processing). Between data points, $\rho_b(T)$ is fit to the form $\rho(T)=\rho_0+\rho_1 T^3$, as suggested by the author. See F. R. Fickett, Phys. Rev. B **2**, 1943 (1971).

[13]A. B. Meador and W. E. Lawrence, Phys. Rev. B **15**, 1850 (1977); see Table IV.

[14]See, for example, D. A. Wharam *et al.* in Ref. 1.

[15]A. Benoit *et al.*, Phys. Rev. Lett. **58**, 2343 (1987).

[16]R. H. Silsbee and Francois Beneu, Phys. Rev. B **27**, 2682 (1983); see Fig. 5.

[17]P. A. M. Benistant *et al.*, J. Phys. F **15**, 2445 (1985); H. Sato and K. Yonemitsu, *ibid.* **16**, 2053 (1986).

[18]N. W. Ashcroft, Philos. Mag. **8**, 2055 (1963).

[19]Mark Johnson, Ph.D. dissertation, Cornell University, Ithaca, NY (1986).